

Active Flash: Towards Energy-Efficient, In-Situ Data Analytics on Extreme-Scale Machines

Devesh Tiwari¹, Simona Boboila², Sudharshan S. Vazhkudai³, Youngjae Kim³,
Xiaosong Ma¹, Peter J. Desnoyers² and Yan Solihin¹

¹North Carolina State University ²Northeastern University ³Oak Ridge National Laboratory
{devesh.dtiwari, ma, solihin}@ncsu.edu, {simona, pjd}@ccs.neu.edu, {vazhkudaiss, kimy1}@ornl.gov

Abstract

Modern scientific discovery is increasingly driven by large-scale supercomputing simulations, followed by data analysis tasks. These data analyses are either performed offline, on smaller-scale clusters, or on the supercomputer itself. Unfortunately, these techniques suffer from performance and energy inefficiencies due to increased data movement between the compute and storage subsystems. Therefore, we propose Active Flash, an in-situ scientific data analysis approach, wherein data analysis is conducted on the solid-state device (SSD), where the data already resides. Our performance and energy models show that Active Flash has the potential to address many of the aforementioned concerns without degrading HPC simulation performance. In addition, we demonstrate an Active Flash prototype built on a commercial SSD controller, which further reaffirms the viability of our proposal.

1 Introduction

High performance computing (HPC) simulations on large-scale supercomputers (e.g., the petascale Jaguar machine, No. 6 on the Top500 list [45] as of June 2012) routinely produce vast amounts of result output data [1, 36]. Examples of such applications include astrophysics (Chimera, Vulcan/2D), climate (POP), combustion (S3D), and fusion (GTC and GYRO) (Table 1). Deriving insights from these simulation results often involves performing a sequence of *data analysis* tasks.

Traditionally, the simulation jobs and data analysis of the simulation outputs are conducted on separate computing resources. Data analysis tasks are run *offline*, on smaller clusters, *after* the completion of the simulation job, as shown in Figure 1. The high-end computing (HEC) machine and the analysis clusters tend to share a high-speed scratch parallel file system (PFS) to access the input/output data.

The reason for using *offline* processing for analysis is that CPU hours are expensive on HEC machines like

Jaguar. Therefore, HPC users generally utilize the allocated CPU hours for FLOP-intensive codes such as the simulation job, instead of data analysis tasks.

Unfortunately, this traditional offline approach suffers from both performance and energy inefficiencies. It requires redundant I/O (simulations write, analyses read), resulting in excessive data movement across the compute and storage subsystems. As we transition from petaflop to exaflop systems, the energy cost due to data movement is predicted to be comparable, if not more than the computing cost [29]. At the same time, technology projections indicate that energy efficiency will become the primary metric for system design, as compute power is expected to increase by 1000× in the next decade with only a 10× increase in power envelope [34]. Therefore, an urgent challenge is to expedite data analysis in an energy-efficient manner, without degrading or interfering with the main simulation computation.

An alternative solution is to perform data analysis on a set of dedicated *analysis nodes*, wherein in-transit output data is analyzed, before being written to the PFS (Figure 1)[22]. Although this eliminates redundant I/O, it uses expensive compute nodes for the relatively less FLOP-intensive data analysis tasks. Moreover, it may even slow down the simulation job due to interference,

Application	Analysis data generation rate (per node)	Checkpoint data generation rate (per node)
CHIMERA	4400 KB/s	4400 KB/s
VULCUN/2D	2.28 KB/s	0.02 KB/s
POP	16.3 KB/s	5.05 KB/s
S3D	170 KB/s	85 KB/s
GTC	14 KB/s	476 KB/s
GYRO	14 KB/s	11.6 KB/s

Table 1: Output characteristics of parallel simulations on Jaguar, amortized over the entire run. Outputs comprise both result (analysis) and recovery (checkpoints) data.

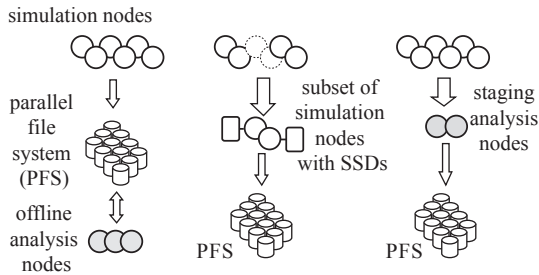


Figure 1: Three approaches to data analysis: (1) *offline* (leftmost), with another cluster for analysis, (2) *active flash* (middle), with analysis on a subset of the simulation nodes with SSDs, and (3) *analysis node* (rightmost), with an extra set of nodes on the same machine for processing.

resulting in inefficient use of expensive resources.

In this paper, we propose a new approach to data analysis in HPC settings, using emerging storage devices such as Solid-State Disk devices (SSDs). SSDs are being deployed on supercomputers (e.g., Tsubame2 [45] and Gordon [32]) due to their higher I/O throughput, and are likely to be an integral part of future storage subsystems. They also have significant compute power on the storage controllers [6] as they are equipped with low-power, ARM-based, multi-core controllers.

We propose *active flash*, a means to exploit the compute power in SSDs for in-situ data analysis. This approach also has the potential to improve performance and yield energy savings since conducting analysis in-situ, where the data already resides, reduces both the associated data transfer latency and energy costs.

The active flash approach resembles prior work in active disks [42, 27], embedding computation in storage devices. The specifics differ significantly, however, due to differences not only in the underlying technology (flash vs. disk), but also in application needs, problem setting and constraints. For example, the compute nodes, performing the HPC simulation, should not observe any perceivable performance degradation due to the active computation on the SSD.

Contributions: The contributions of this work are as follows: (1) We present detailed energy and performance models for the active flash, offline, and analysis node approaches (the three modes shown in Figure 1). We evaluate them using realistic measurements both from Jaguar and data rates from several leadership applications. We model the conditions under which it is feasible to offload data analytics to SSD controllers, showing that active flash can execute many popular data analytics kernels in the background without degrading simulation performance, and provides better performance and energy consumption than alternative approaches. (2) We have built an active flash prototype on the Jasmine OpenSSD development platform [26], ex-

tending the OpenSSD flash translation layer (FTL) with data analysis functions, demonstrating the feasibility of adding active flash functionality without requiring any hardware changes. (3) Via modeling, simulation-based verification, and our prototype, we have shown that active flash is a cost-effective and energy-efficient execution model for in-situ scientific data analysis.

2 Background

SSD-based Staging Area for HPC Simulation Output: HPC simulations produce tens of TBs of output data, composed of *analysis data* and *checkpoint data*, both written at periodic intervals. For instance, a GTC application (Table 1) run using 18,000 compute nodes (225,000 cores) on Jaguar produces 30TB of output every hour. Analysis data forms the input to post-processing, analytics, and visualization. Checkpoint data stores a snapshot of the execution’s state, for future restart purposes.

Exascale projections [34] indicate that emerging application data rates will exert a tremendous amount of pressure on the PFS, exposing the I/O bottleneck dramatically [1, 34]. Consequently, the HPC community has been investigating SSD-based solutions to help alleviate this I/O bandwidth bottleneck. Several studies have proposed the use of compute node-local SSDs as an intermediate storage buffer that can store the output data, and help recover from a failed state [10, 40, 12, 15, 37]. We refer to this collective SSD space as the *staging area*.

In this paper, we argue that performing on-the-fly data analysis on the *SSDs in the staging area* will be cost-effective, and energy-efficient. Given the massive scale of modern supercomputers, it may not be cost-effective to deploy SSDs on each and every compute node. A more realistic assumption is that they can only be attached to a subset of the nodes. *In the next section, we will investigate the following questions: how many SSDs should be deployed in the staging area to meet the data requirements of applications, and are they sufficient to perform active processing without degrading the performance of the main simulation?*

Enabling Trends for Active Flash: While SSDs are being deployed on HEC machines to cater to growing I/O demands, we highlight the following trends that make it amenable for active processing.

High I/O throughput and internal bandwidth: SSDs offer high I/O throughput and internal bandwidth due to interleaving techniques over multiple channels and flash chips. This bandwidth is likely to increase with devices possessing more channels or flash chips with higher-speed interfaces.

Availability of spare cycles on the SSD controller: HPC workloads are bursty, with distinct compute and I/O phases. Typically, a busy short phase of I/O activ-

ity is followed by a long phase of computation [16, 28]. Further, the I/O activity recurs periodically (e.g., once every hour in the GTC application), and the total time spent on I/O is usually low (below 5% [1]). Even some enterprise workloads exhibit idle periods between their I/O bursts [31, 30]. Such workloads expose spare cycles available on the SSD controller, making it a suitable candidate for offloading data analysis tasks.

Multi-core SSD controllers: Recently marketed SSDs are equipped with fairly powerful mobile cores, and even multi-core controllers (e.g. a 4-core 780 MHz controller on the OCZ RevoDrive X2 [33]). Multi-core SSD controllers are likely to become more common place, largely due to Moore’s law, and hence the available idle time on the SSD controllers will increase as well.

Alternative Approach Using Analysis Nodes: One alternative is to perform data analysis on dedicated low-power processors, similar to the wimpy node architecture [11]. Fortunately, these low-power cores are *already* available on the SSD controllers being deployed on large-scale machines. Further, SSDs offer better I/O throughput and storage space. We argue that piggybacking data analysis on existing SSD deployment eliminates additional effort and cost associated with procuring and installing wimpy nodes on the supercomputer’s interconnect. Moreover, the high internal bandwidth of SSDs makes it more attractive for embedding computation.

Another alternative is the *analysis nodes* approach. As discussed in Section 1, running the data analysis tasks on the high performance compute nodes (*simulation nodes*), along with the HPC simulation process, may cause interference and degrade the performance of simulation process. Therefore, we model a more generalized analysis node approach in this paper, where we allocate a set of dedicated simulation nodes, solely for in-situ data analysis. We model this approach and compare it against active flash, and offline techniques.

3 Modeling Data Analysis

In this section, we study the performance and energy tradeoffs of *active flash*, *offline*, and *analysis node* approaches. With the *active flash* approach, we propose to conduct data analysis on the storage device controller (SSD controller) itself. With the traditional *offline* approach, data analysis or post-processing is performed on a set of compute nodes after the simulation finishes on a supercomputer. These *postprocessing compute nodes* can be allocated from the same supercomputer or from an offline cluster that shares a common PFS with the supercomputer. Finally, with the *analysis node* approach, data analytics is performed on a set of compute nodes, on the same simulation machine, while the output data is in-transit from simulation nodes to the PFS.

3.1 Active Flash

With active flash, we perform analysis on the output data, utilizing the idle cycles of the SSD controller to operate on temporary, SSD-resident data. We assess the feasibility of this new execution paradigm by developing an analytical model to examine the aggregate processing power and energy consumption of distributed SSD devices.

3.1.1 SSD Staging Ratio

We assume that SSDs are provisioned in HEC machines based on typical I/O demands and not based on data analysis requirements. The factors considered include capacity, performance, and write durability.

With this assumption, the total SSD storage required is determined by the following parameters: (1) the per-compute-node data production rate for both analysis and checkpoint data, denoted as λ_a and λ_c respectively, (2) the length of an output iteration (the time between two periodic output operations), t_{iter} , (3) the total number of compute nodes in the system, N , and (4) the number of checkpoints retained in the staging area, num_{chkpts} . Below we derive the required *staging ratio*, under different constraints.

Capacity: Intuitively, given the capacity of an SSD, and an application’s data production rate and frequency, the SSD can only hold the data produced by a certain number of compute nodes. We refer to this as the capacity based staging ratio, $R_{capacity}$. More formally, taking into account a certain over-provisioning factor, f_{op} , for the SSD space, the total SSD storage requirement at any given time can be estimated as $f_{op} \cdot (\lambda_a + num_{chkpts} \cdot \lambda_c) \cdot N \cdot t_{iter}$. The number of SSDs is the total SSD storage requirement divided by the capacity of one SSD, C_{SSD} . Consequently, the *maximum staging ratio* (the maximum number of compute nodes sharing one SSD) can be calculated as:

$$R_{capacity} = \frac{C_{SSD}}{f_{op} \cdot (\lambda_a + num_{chkpts} \cdot \lambda_c) \cdot t_{iter}} \quad (1)$$

Performance: There are two kinds of performance constraints. First, the aggregate bandwidth to all SSDs must be at least that of the PFS itself, otherwise the application will invariably suffer a slowdown. If the interface bandwidth between the simulation node and SSD is $BW_{sim-SSD}$, the maximum staging ratio can be stated as follows:

$$R_{bandwidth} = \frac{BW_{sim-SSD}}{\frac{BW_{PFS}}{N}} \quad (2)$$

Second, a key objective of SSD deployment in HPC is to expedite application recovery by enabling faster reads of the checkpoint data. Therefore, the compute node should be able to read the checkpoint snapshot data from the SSD within a certain duration, compared to the output frequency. We refer to this as the “*restart I/O threshold*”

fraction”, ($f_{restart}$), which expresses the desired I/O time for recovery, as a fraction of the checkpoint interval; typical values range from 0.03 to 0.05 [1]. The resulting constraint on the staging ratio is thus:

$$R_{restart} = \frac{f_{restart} \cdot BW_{sim-SSD}}{\lambda_c} \quad (3)$$

Write-endurance: An additional constraint is imposed by the finite write endurance of SSDs. Large-scale HPC systems are typically upgraded at regular intervals, and the minimum lifetime of any system component is dictated by the interval between two system upgrades (U_{time}). If we measure the write endurance $W_{endurance}$ of an SSD by the maximum number of bytes which may be safely written over its lifetime, then the write endurance limit on staging ratio is:

$$R_{endurance} = \frac{W_{endurance}}{(\lambda_a + \lambda_c) \cdot U_{time}} \quad (4)$$

The final staging ratio is determined by the most restrictive constraint of all:

$$R_{SSD} = \min(R_{capacity}, R_{bandwidth}, R_{restart}, R_{endurance}) \quad (5)$$

Observation 1 *Even without taking active computation into account, deciding staging ratio for SSD deployment is non-trivial. More SSDs are required (i.e. lower staging ratio) when output data production rate, PFS bandwidth, and system upgrade time are high, while higher write-endurance, SSD bandwidth, and allowable I/O overhead require fewer SSDs (i.e. higher staging ratio).*

3.1.2 Performance Model

Given an SSD deployment, with a staging ratio determined by the above constraints, we derive a performance model to study which data analytics kernels can be offloaded to the SSD without degrading the performance of the main simulation. For active computation to happen in the background without degrading the performance of the main simulation, the summation of the time taken to perform data analysis on the SSD controller, and the time taken to drain both the analysis and checkpoint data to the PFS, should be less than the output frequency of the application. Therefore, the data analysis kernels that can be offloaded depends on the compute throughput of the analysis kernel, the application’s data production rate, staging ratio, and other system specific characteristics (e.g., SSD internal bandwidth, and PFS bandwidth among other things). In the following discussion, we derive a set of equations, describing the relationship between these factors.

Once the analysis data arrives at the SSD in the staging area, active computation involves the following data transfers: (1) from the flash memory to the flash chip controller at the SSD internal bandwidth, BW_{fm2c} , and (2) from the flash chip controller to the on-device DRAM at bandwidth, BW_{c2m} (see Figure 2 for a detailed view

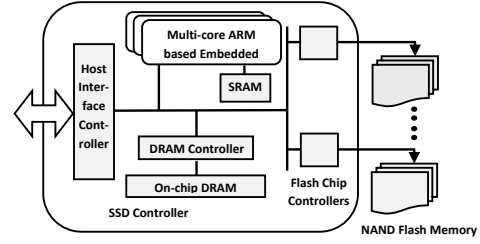


Figure 2: Detailed view of the SSD controller

of the SSD controller). We use $T_{SSD,k}$ to denote the data processing throughput of a single active flash device, running the data analysis kernel, k . Certain data analytics kernels (e.g., statistical summaries) may even reduce the analysis data by some factor α . The SSD is responsible for writing the analysis data (possibly reduced) and checkpoint data to the PFS, consuming an appropriate share of the aggregate file system bandwidth BW_{PFS} . Processing plus output time for analysis results per checkpoint interval is thus:

$$t_a = R_{SSD} \cdot \lambda_a \cdot \left(\frac{1}{BW_{fm2c}} + \frac{1}{BW_{c2m}} + \frac{1}{T_{SSD,k}} + \frac{\alpha}{\frac{R_{SSD}}{N} \cdot BW_{PFS}} \right) \cdot t_{iter} \quad (6)$$

and the checkpoint data output time is as follows:

$$t_c = \frac{R_{SSD} \cdot \lambda_c}{\frac{R_{SSD}}{N} \cdot BW_{PFS}} \cdot t_{iter} \quad (7)$$

While the draining of the staged checkpoint data to the PFS can overlap with the processing of analysis data, we conservatively assume that these two tasks are carried out sequentially on the same SSD controller core.

To account for the overhead of transferring data over the interconnect from SSDs to I/O nodes, we next model the interconnect transfer time. We assume that the mean distance from a staging node to the nearest I/O node is hop distance, d , and that is the same as the mean distance from a simulation node to the nearest I/O node.

Assuming wormhole routing [18]) with packets segmented into m -byte *flits*, and interconnect bandwidth (with no contention) of $BW_{idlelink}$, the total data transfer time within a single output interval t_{iter} is:

$$t_i = \frac{m}{BW_{idlelink}} \cdot d + \frac{R_{SSD} \cdot (\alpha \cdot \lambda_a + \lambda_c)}{BW_{idlelink}} \cdot t_{iter} \quad (8)$$

$BW_{idlelink}$ is an optimistic bandwidth estimate for the interconnect latency, which may potentially favor our active computation approach; we thus model contention in order to provide a conservative transfer time estimate.

The interconnect contention ratio is the mean number of nodes sharing one link. Assuming in the worst case that each node sends a message to its farthest neighbor in the interconnection network, we have a total of $N \cdot d_{max}$ messages, where N is the total number of nodes and d_{max} is the network diameter. If the total number of links is

L , then per-link contention is $\frac{N \cdot d_{max}}{L}$. Thus, the effective interconnect bandwidth can be expressed as $\frac{BW_{idlelink} \cdot L}{N \cdot d_{max}}$, and Equation 8 can be re-written as follows:

$$t_i = \frac{1}{BW_{busylink}} \cdot (m \cdot d + R_{SSD} \cdot t_{iter} \cdot (\alpha \cdot \lambda_a + \lambda_c)) \quad (9)$$

where

$$BW_{busylink} = \frac{BW_{idlelink} \cdot L}{N \cdot d_{max}}$$

The diameter, d_{max} , of an interconnect and the total number of links can be determined from the topology.

For the active flash approach to be feasible, the device needs to process and output the data from the S simulation nodes before the next I/O iteration, i.e., consuming data at a rate faster than its generation:

$$t_a + t_c + t_i < t_{iter} \quad (10)$$

Solving the inequality 10, we arrive at the minimum processing throughput required for an analytics kernel, k to be placed on the flash device:

$$T_{SSD,k} > \frac{\lambda_a \cdot R_{SSD}}{1 - \lambda_a \cdot R_{SSD} \cdot \left(\frac{1}{BW_{fm2c}} + \frac{1}{BW_{c2m}} \right) - \frac{N \cdot (\alpha \cdot \lambda_a + \lambda_c)}{BW_{PFS}} - \frac{t_i}{t_{iter}}} \quad (11)$$

In Section 5, we use this equation to evaluate the performance feasibility of active flash for a set of representative large-scale applications and data analytics kernels.

Observation 2 *Multiple factors determine which kernels may be offloaded to the SSD without degrading simulation performance. Increases in either PFS or internal SSD bandwidth allow more computationally-intensive kernels to be offloaded, while higher staging ratios and data production rates decrease the amount of computation which may be offloaded.*

3.1.3 Energy Model

Total energy consumed by the active flash approach ($E_{active-flash}$) can be expressed as the summation of the data movement energy expense in the interconnect ($E_{interconnect}$), and the energy consumed by all of the SSDs in the staging area (E_{SSD}), for the entire duration of the application run:

$$E_{active-flash} = E_{interconnect} + E_{SSD} \quad (12)$$

First, we model the interconnect energy as the data movement energy overhead for a given number of hops. If $e(h)$ represents the energy to transfer a unit amount of data across h hops, then we can express the total data movement energy cost as:

$$E_{interconnect} = t_{sim} \cdot N \cdot (e(d_s) \cdot (\lambda_a + \lambda_c) + e(d) \cdot (\alpha \cdot \lambda_a + \lambda_c)) \quad (13)$$

where d_s is the number of hops from the simulation node to its nearest staging node. (Recall that d is the distance from a staging node to the nearest I/O node.)

The energy consumed by the SSDs is:

$$E_{SSD} = E_{busySSD} + E_{idleSSD} - E_{iosaving} \quad (14)$$

where $E_{busySSD}$, energy consumed during the SSD busy time, is the summation of (1) the energy to transfer data from the simulation nodes to the SSDs ($E_{sim-SSD}$), (2) the energy used while processing analysis data ($E_{activeSSD}$), and (3) the energy to transfer data to the PFS ($E_{SSD-PFS}$).

$E_{idleSSD}$, in turn, is the energy consumed by the SSD in the idle state (when it is not performing I/O or computation). Finally, higher I/O bandwidth due to SSDs may reduce the time spent waiting for I/O at the simulation nodes; the resulting reduction in energy consumption at the simulation nodes is denoted by $E_{iosaving}$.

Next, we estimate each component of the SSD busy time ($E_{busySSD}$) individually. Let P_{busy}^{SSD} and P_{idle}^{SSD} be the SSD busy and idle power levels, respectively, and t_{sim} the total simulation computation time for a single application run.

$E_{sim-SSD}$ is the total time ($t_{transfer}$) to transfer data from the simulation nodes to the SSDs in the staging area, times the power P_{busy}^{SSD} . Total data transferred is:

$$data_{total} = N \cdot (\lambda_a + \lambda_c) \cdot t_{sim}$$

Then, the $t_{transfer}$ is equal to:

$$\left(\frac{1}{BW_{sim-SSD}} + \frac{1}{BW_{busylink}} \right) \cdot data_{total}$$

The total energy consumed by the SSDs during the data transfer from the simulation nodes to the SSDs can then be expressed as:

$$E_{sim-SSD} = P_{busy}^{SSD} \cdot t_{transfer} \quad (15)$$

Similarly, the time taken to post-process, $t_{activecompute}$, is equal to:

$$N \cdot \lambda_a \cdot t_{sim} \left(\frac{1}{BW_{fm2c}} + \frac{1}{BW_{c2m}} + \frac{1}{T_{SSD,k}} \right)$$

and the total energy consumed by the SSDs during data analysis is:

$$E_{activeSSD} = P_{busy}^{SSD} \cdot t_{activecompute} \quad (16)$$

After data analysis tasks, both checkpoint and analysis data are written to the PFS by the SSDs. Accounting for both PFS transfer and interconnect latency, the energy cost is:

$$E_{SSD-PFS} = P_{busy}^{SSD} \cdot data_{total} \cdot \left(\frac{1}{BW_{PFS}} + \frac{1}{BW_{busylink}} \right) \quad (17)$$

Finally, the idle energy consumption can be calculated from the estimated total idle time, utilizing the busy time estimate above:

$$E_{idleSSD} = P_{idle}^{SSD} \cdot \left(\frac{N}{R_{SSD}} \cdot t_{sim} - \frac{E_{activeSSD} + E_{SSD-PFS}}{P_{busy}^{SSD}} \right) \quad (18)$$

The busy time involved in $E_{sim-SSD}$ is not subtracted in the equation above, unlike the other two components. This is because both the CPUs and the SSDs are involved in the data transfer, which is not a part of t_{sim} , and does not perform data generation.

We estimate the per-node idle time reduction as

$$T_{iosaving} = \frac{N \cdot (\lambda_a + \lambda_c)}{BW_{PFS}} - (R_{SSD} \cdot (\lambda_a + \lambda_c)) \cdot \left(\frac{1}{BW_{sim-SSD}} + \frac{1}{BW_{busylink}} \right)$$

Therefore, the energy savings on the simulation nodes, over the entire application run is:

$$E_{iosaving} = N \cdot T_{iosaving} \cdot t_{sim} \cdot P_{idle}^{server} \quad (19)$$

Observation 3 *Energy spent during the SSD busy time is dependent on the total amount of work performed and the data transferred, and thus independent of the staging ratio (i.e. the number of SSDs deployed). In contrast, idle SSD energy costs and energy savings on the simulation nodes vary with the staging ratio.*

3.2 Modeling Offline Processing

With the offline approach, compute nodes on the analysis cluster need to read only the analysis data and write the results according to their share of the whole data, i.e., $\frac{N \cdot \lambda_a}{M}$, assuming M nodes are used to perform offline analysis. Similarly, each of the M nodes need to process the data at the processing rate, $T_{server,k}$, for a given kernel k . Again, we assume that each node gets its appropriate share of the PFS bandwidth $\frac{1}{N} \cdot BW_{PFS}$. The interconnect latency would be equal to $\frac{N \cdot \lambda_a}{M \cdot BW_{busylink}}$. The following equation captures the runtime of the offline analysis:

$$T_{offline} = \frac{N \cdot \lambda_a \cdot t_{sim}}{M \cdot T_{server,k}} + (1 + \alpha) \cdot \left(\frac{N \cdot \lambda_a \cdot t_{sim}}{M} \right) \cdot \left(\frac{N}{BW_{PFS}} + \frac{1}{BW_{busylink}} \right) \quad (20)$$

In some cases, analysis data is transferred over the wide area network for processing, resulting in more performance and energy penalty than what our optimistic model estimates.

Next, we model the energy cost of offline processing. We charge only idle power for the compute servers while they read and write the analysis data, and account for busy power during data analysis. We can obtain this by multiplying Equation 20 by P_{idle}^{server} for the reading and writing part of the process, and multiplying by P_{busy}^{server} for the analysis part of the process.

There are various topologies which could be used for the offline approach, making estimates of interconnect energy cost difficult. We therefore conservatively ignore the cost of moving data to an offline compute cluster when comparing to our active flash approach, giving a total energy cost of:

$$E_{offline} = P_{idle}^{server} \cdot (1 + \alpha) \cdot \left(\frac{N^2 \cdot \lambda_a \cdot t_{sim}}{BW_{PFS}} + \frac{N \cdot \lambda_a \cdot t_{sim}}{BW_{busylink}} \right) + P_{busy}^{server} \cdot \frac{N \cdot \lambda_a \cdot t_{sim}}{T_{server,k}} \quad (21)$$

Observation 4 *The energy cost of offline processing does not depend on the number of offline nodes, but only on the total amount of data to be read and processed.*

3.3 Modeling the Analysis Node Approach

Much like the case of SSD deployment, we begin by determining the staging ratio for analysis node deployment, based on capacity and bandwidth constraints. The capacity constraint here refers to the memory capacity (C_{mem}) on the analysis node, and the bandwidth constraint corresponds to the memory bandwidth (BW_{mem}) instead of the host to SSD bandwidth.

We assume that all simulation output—both checkpoint data and analysis input—is transferred to the analysis nodes, as is done by libraries such as ADIOS [22], as the resulting increase in checkpoint write bandwidth allows the simulation nodes to progress faster.

Equations 1, 2, and 5 are thus changed as follows:

$$R_{capacity} = \frac{C_{mem}}{f_{op} \cdot (\lambda_a + num_{chkpts} \cdot \lambda_c) \cdot t_{iter}} \quad (22)$$

$$R_{bandwidth} = \frac{N}{BW_{PFS}} \cdot BW_{mem} \quad (23)$$

$$R_{a,node} = \min(R_{capacity}, R_{bandwidth}) \quad (24)$$

where subscript $a,node$ refers to the analysis node approach. Similarly, Equations 6, 7, and 9 can be modified to estimate the data analysis time, output time, and the interconnect latency:

$$t_a = R_{a,node} \cdot \lambda_a \left(\frac{1}{T_{a,node,k}} + \frac{\alpha}{\frac{R_{a,node}}{N} \cdot BW_{PFS}} \right) \cdot t_{iter} \quad (25)$$

where $T_{a,node,k}$ is the throughput required to run the data analysis kernel, k on the analysis node.

$$t_c = \frac{R_{a,node} \cdot \lambda_c}{\frac{R_{a,node}}{N} \cdot BW_{PFS}} \cdot t_{iter} \quad (26)$$

$$t_i = \frac{1}{BW_{busylink}} \cdot (m \cdot d + R_{a,node} \cdot t_{iter} (\alpha \lambda_a + \lambda_c)) \quad (27)$$

Similar to the active flash model, we can derive the minimum throughput required for the analytics kernels that can be offloaded to the analysis nodes:

$$T_{a,node,k} > \quad (28)$$

$$\frac{\lambda_a \cdot R_{a,node}}{1 - \frac{N \cdot (\alpha \lambda_a + \lambda_c)}{BW_{PFS}} - \frac{1}{BW_{busylink}} \left(\frac{m \cdot d}{t_{iter}} + R_{a,node} \cdot (\alpha \lambda_a + \lambda_c) \right)}$$

Next, we account for the energy overhead of the different components, starting with data movement costs, which are:

$$E_{interconnect} = t_{sim} \cdot N \cdot (e(d_s^{a,node}) \cdot (\lambda_a + \lambda_c) + e(d) \cdot (\alpha \cdot \lambda_a + \lambda_c)) \quad (29)$$

where $d_s^{a,node}$ is the average number of hops from the simulation nodes to the analysis nodes. Next, we account for the energy cost when analysis nodes are busy.

This comprises of three components: (1) transferring data from the simulation nodes to the data analysis node (E_{sim-a_node}), (2) processing the analysis data (E_{a_node}), and (3) transferring the data to the PFS ($E_{a_node-PFS}$).

Let $P_{busy}^{a_node}$ and $P_{idle}^{a_node}$ be the data analysis node's busy and idle power level, respectively. Then, we can modify Equations 15 to 19 to get the corresponding equations for data analysis energy overheads:

$$E_{sim-a_node} = P_{busy}^{a_node} \cdot \left(\frac{1}{BW_{mem}} + \frac{1}{BW_{busylink}} \right) \cdot data_{total} \quad (30)$$

$$E_{a_node} = \frac{P_{busy}^{a_node} \cdot N \cdot \lambda_a}{T_{a_node.k}} \cdot t_{sim} \quad (31)$$

$$E_{a_node-PFS} = \quad (32)$$

$$P_{busy}^{a_node} \cdot data_{total} \cdot \left(\frac{1}{BW_{PFS}} + \frac{1}{BW_{busylink}} \right) \quad (33)$$

$$E_{idle-a_node} = \frac{P_{idle}^{a_node}}{R_{a_node}} \cdot \left(\frac{N}{R_{a_node}} \cdot t_{sim} - \frac{E_{a_node} + E_{a_node-PFS}}{P_{busy}^{a_node}} \right)$$

Finally, we estimate the per simulation node idle time reduction due to analysis nodes as:

$$T_{iosaving-a_node} = \frac{N \cdot (\lambda_a + \lambda_c)}{BW_{PFS}} - (R_{a_node} \cdot (\lambda_a + \lambda_c)) \cdot \left(\frac{1}{BW_{mem}} + \frac{1}{BW_{busylink}} \right)$$

and total energy savings for this approach is:

$$E_{iosaving-a_node} = N \cdot T_{iosaving-a_node} \cdot t_{sim} \cdot P_{idle}^{sim} \quad (34)$$

4 Experimental Methodology

We evaluate our models using the data production rates from extreme-scale applications on the Jaguar machine at ORNL (Table 1).

Our model is generic and applies to common super-computer configurations seen today. Our evaluation is driven by parameters from the Cray XT5 Jaguar super-computer [8], as shown in Table 2. In the current SSD landscape, there is no support for active computation on the device. To study the viability of active flash, we model after a contemporary SSD such as Samsung PM830, which has a multicore SSD controller based on the ARM processor [6]. Although such a controller has three ARM-based cores, we adopt a conservative approach, and propose to use only one core for active computation, while leaving the other cores free for typical SSD activities (e.g. error-checking, garbage collection). In the future, more cores are likely to be placed on the same chip, making active computation more promising than what is projected in this study.

To emulate the computing speed of the ARM-based SSD controller, we use an ARM Cortex-A9 processor in the Pandaboard mobile software development platform [38]. We model the data transfer times as follows. We assume 8 flash memory channels, each with 40MB/s

No. of compute nodes (N)	18,000
PFS bandwidth (BW_{PFS})	240 GB/s [35]
Output frequency (t_{iter})	1 hour
Simulation duration (t_{sim})	24 hours
Overprovisioning factor (f_{op})	1.50
Data reduction factor (α)	1 (no reduction)
Time between upgrades (U_{time})	2 years
Restart I/O threshold ($f_{restart}$)	0.05 [1]
Interconnect bandwidth ($BW_{busylink}$)	814 MB/s
Flit size (m)	32 bytes
Hop count ($d, d_s, d_s^{a_node}$)	3 hops, 1.5 hops, 1.5 hops
$e(d), e(d_s), e(d_s^{a_node})$	10 pJ/bit, 5 pJ/bit, 5 pJ/bit [9, 14]
SSD model	Samsung PM830
$BW_{sim-ssd}$	400 MB/s [20]
BW_{fm2c}	320 MB/s [20]
BW_{c2m}	3.2GB/s [4]
SSD power (P_{busy}, P_{idle})	3 W, .09 W [6]
SSD write endurance ($W_{endurance}$)	300 TB written [6]
Offline model / analysis node model	2 Intel Core i7 [3]
BW_{mem}	30 GB/s
Node power (P_{busy}, P_{idle})	190 W, 63 W
Price: SSD (64 GB), node (2 quad cores), DRAM (64 GB)	\$ 100 [7], \$ 610 [5], \$ 400 [2]

Table 2: Parameters for performance and energy models.

bandwidth, to transfer data from the NAND Flash to the chip controller (BW_{fm2c}) [20]. Our numbers are conservative, and modern devices usually have higher channel bandwidth or more channels. Similarly, while the DDR2 SDRAM cache used in these SSDs may have a bandwidth of up to 5.3GB/s [4], we conservatively set BW_{c2m} to 3.2GB/s.

For a comparison with the offline and analysis nodes models, we use two Intel Core i7 2600 processor (3.4GHz with eight hardware contexts) [3] as the data processing node. We use an input file of 100MB to measure the analysis throughput.

The chosen data analytics kernels cover a wide variety of representative analytics operations on scientific data, including pattern matching, clustering, changing data layout, and compression [23, 24, 21]. We measured their processing throughput on both the ARM-based SSD controller and the Intel server (Table 4). Note that the throughput of the analysis kernels may be input-dependent as well (e.g. number of clusters, dimensions, and search expressions). Therefore, choosing a wide variety of kernels, whose throughput varies from less than one MB/s to a few GB/s helps better understand the limits, and the potential of active flash.

For energy calculations we use the thermal design power (TDP) of 190W ($2 \times 95W$ per machine) as the busy-state power for each offline node; we conservatively estimate idle power at one third of TDP and cool-

Data Analytics Kernels	ARM Cortex-A9	Intel core i7-2600
Statistics (mean)	416 MB/s	54.2 GB/s
Pattern Matching (grep)	123 MB/s	9.65 GB/s
Data formatting (transpose)	76 MB/s	3.25 GB/s
Dim. reduction (PCA)	10.2 MB/s	549 MB/s
Compression (gzip)	4.1 MB/s	225 MB/s
Dedup. (Rabin fingerprint)	1.81 MB/s	143 MB/s
Clustering (k-means)	0.91 MB/s	27.3 MB/s

Table 3: Processing throughput of common data analytics kernels on different devices. Our offline compute node consists of two Intel core i7-2600 machines.

ing cost as zero.

In addition, we ignore the power required for memory and network traffic for the offline approach, which is clearly higher compared to active flash due to additional reading of the analysis data.

We computed the hop counts, d for Jaguar as follows. Jaguar has 200 cabinets in 8 rows and 25 columns, with 3 cages per cabinet, 8 blades per cage, and four compute nodes per blade. Every node is connected via the 3D torus Cray Gemini network, with routing on X, Y, Z directions [19]: X is across cabinets within a row, Y is across cabinets within a column, and Z is across nodes within a cabinet. Average cable lengths are 1.8 m and 7.5 m for the X and Y directions respectively. Based on the coordinate information, we can infer node-to-node hop count in distance, and also determine the number of cabinets traversed. To account for the energy cost in our experiments, we are particularly interested in the hop distance from the compute nodes to the I/O nodes and consequently, the number of cabinets traversed. We estimate d_s and $d_s^{a,node}$ to be half of d (Table 2). This, however, is a conservative estimate since the number of analysis nodes or SSDs (e.g., at a staging ratio of 10) is approximately 9 times the number of I/O nodes (192) in Jaguar.

We have validated the busy link bandwidth model, $BW_{busylink}$, against the actual link bandwidth measurement on Jaguar by performing all-to-all MPI communication between N node pairs; measured busy link bandwidth based on 1024 nodes is 814 MB/s.

5 Evaluation

Our evaluation aims to answer three questions: (1) What is the staging ratio for SSD provisioning, based on different constraints for representative applications? (2) Will these staging ratios support *in-situ* data processing on SSDs? (3) If so, what energy savings may be achieved with active flash?

Staging ratio: Table 4 shows the staging ratio for the active flash, and the analysis node models, based on constraints from Equations 1-4 and 22-23; higher staging

Active Flash Model						
	CHIMERA	VULCAN	POP	S3D	GTC	GYRO
$R_{capacity}(32GB)$	1	2571	233	18	6	166
$R_{capacity}(64GB)$	1	4500	461	36	12	333
$R_{bandwidth}$	29	29	29	29	29	29
$R_{endurance}$	1	2268	245	20	10	204
$R_{restart}$	4	896218	4054	240	42	1758
Analysis Node Model						
	CHIMERA	VULCAN	POP	S3D	GTC	GYRO
$R_{capacity}(16GB)$	1	1285	117	9	3	83
$R_{capacity}(32GB)$	1	2571	233	18	6	166
$R_{capacity}(64GB)$	1	4500	461	36	12	333
$R_{bandwidth}$	2250	2250	2250	2250	2250	2250

Table 4: Staging ratio derived from capacity, bandwidth, and endurance and restart (flash only) constraints for applications on Jaguar. The most restrictive ratio is shown in bold.

ratios correspond to more compute nodes per SSD or analysis node. Capacity constraints are identical for both models, while bandwidth constraints differ due to higher memory bandwidth (for analysis nodes) than SSD bandwidth (for active flash), and are application independent constants of 2250, and 29, respectively. For active flash the bandwidth constraint is most restrictive for applications with high data rates relative to overall data volume, capacity is not restrictive for 64GB SSDs, and write endurance is a limitation for applications like S3D, and GTC with large output volumes.

Inference: *The limiting factor for active flash seems to be workload dependent, whereas capacity is the overriding concern for analysis nodes.*

Infrastructure cost: As stated above (Section 2), SSDs are currently deployed in HEC systems as burst buffers to alleviate I/O bandwidth bottlenecks when checkpointing. As active flash piggybacks computation on this *existing infrastructure*, we argue that its cost may be ignored, unlike that of analysis nodes; however to be conservative our analysis considers both costs in Figure 3(a) (cost details in Table 2). At low staging ratios the analysis node approach is rather expensive—e.g. \$1,818,000 to provision Jaguar with 64 GB DRAM analysis nodes at a staging ratio of 10, vs. \$180,000 for SSDs at the same ratio. However, analysis nodes might enjoy a higher staging ratio in certain cases due to its higher memory bandwidth.

One example is the application POP, where the staging ratio is limited to 29 by bandwidth for active flash, but is capacity-limited to 461 for analysis nodes (Table 4). Provisioning cost is estimated at roughly \$62,000 and \$39,390 for active flash and analysis nodes, respectively.

Inference: *Analysis nodes can sustain a higher staging ratio at higher capacities, which can help reduce the infrastructure costs. However, as active flash piggybacks on existing infrastructure, its cost is already paid for.*

Feasibility analysis: A higher staging ratio lowers the infrastructure cost, but not all analysis kernels are feasible above certain staging ratios. Figure 3(b) shows the

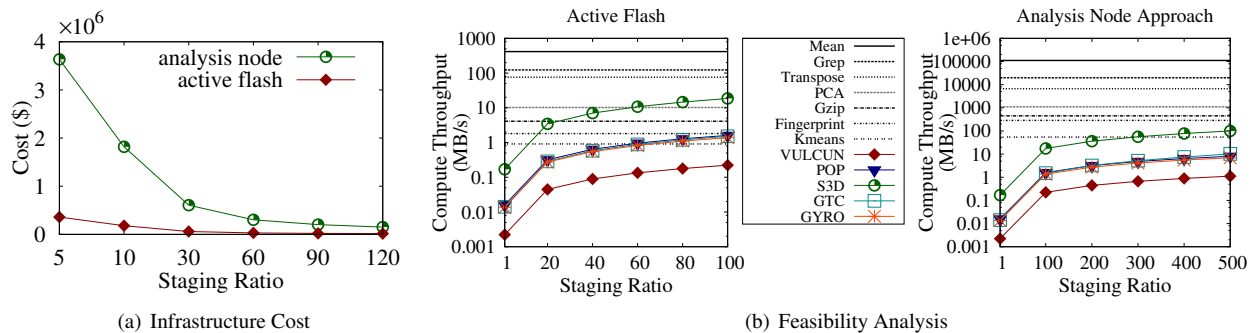


Figure 3: (a) Cost of provisioning SSDs, and analysis nodes. The SSD capacity is 64GB; the analysis node is a dual quad-core machine with 64GB of DRAM. (b) Feasibility of running analysis kernels using different staging ratios. A kernel line *higher* than a dot point on the application’s slope line is *suitable* for active flash (left figure), and the analysis node approach (right figure).

computational throughput of the analysis kernels as flat horizontal lines and the application throughput requirement as sloped lines with dots. A data analysis kernel is able to run on the SSD without any penalty to the simulation performance if its computational throughput is higher than the required throughput of the application ($T_{SSD,k}$ in Equation 12, and $T_{a,node,k}$ in Equation 28). As the staging ratio increases, the processing requirements for both active flash devices and analysis nodes increase.

For example, all of the data analysis kernels can be run on active flash (left graph in Figure 3(b)) for the fusion application *S3D*, when the staging ratio is 5, i.e. 3,600 SSDs for 18,000 compute nodes. As we increase the staging ratio to 50, the *gzip*, *fingerprinting*, and *kmeans* analysis kernels cannot be run on the SSD for this application’s output, as the threshold throughput of *S3D* is *higher* than the compute throughput of these kernels. Figure 3(b) shows that a staging ratio as high as 300 can accommodate all data analysis kernels for most applications, with the exception of the *S3D* application.

For the analysis node model with 64GB of DRAM, a staging ratio of 10 can accommodate all of the kernels for all of the applications, but incurs \$1.8M infrastructure cost. To reduce provisioning costs the staging ratio may be increased beyond this point, reducing the number of analysis kernels which may be used with certain applications. For example, if the staging ratio is increased to 30, the cost falls 67%, to \$606,000, while eliminating support for running data analysis kernels on the output of *GTC* (Table 4).

Inference: *Both active flash and analysis node techniques can support most of the kernels and applications at low staging ratios, but at a higher infrastructure cost. High infrastructure cost can be reduced by increasing the staging ratio, but that scarifies the analysis kernels that can be run on active flash or analysis nodes.*

Energy consumption: Next, we discuss the energy consumption of the models, and its effect on the overall cost. Figure 4 shows the energy costs of active flash, offline, and analysis nodes. We assume a staging ratio of 10, al-

lowing almost all application/analysis kernel pairings to be executed except for *CHIMERA*(Figure 3(b)). Additionally, active flash can not support *kmeans* kernel for *S3D* application. For this ratio we need 1800 staging or analysis nodes, each with 64GB of SSD or DRAM, to accommodate the next most restrictive application, *GTC*.

We define the configuration $baseline_{PFS}$ ($y = 0$) to be the case where the simulation is run without SSDs: all checkpoint and output data are written to the PFS, and no further data analysis is performed after simulation. Results are given as the difference between energy usage for a configuration vs. that for $baseline_{PFS}$; negative numbers indicate energy savings. We observe that deploying SSDs just for higher I/O throughput ($baseline_{SSD}$, the dotted horizontal line in Figure 4), saves significant energy by shortening application run time.

It is not surprising that active flash consumes extra energy compared to $baseline_{SSD}$; however, it still results in savings compared to $baseline_{PFS}$ for almost all application / kernel pairs (except *VULCUN*, which performs little I/O). In contrast, the offline model consumes more energy due to the I/O wait time on the offline compute nodes. For example, for *S3D* with *fingerprinting*, active flash conserves more than 800 kWh per simulation run vs. offline processing, due to the volume of analysis data.

Active flash also results in significant energy savings over use of analysis nodes. For the same *S3D* with *fingerprinting*, we observe more than 2500 kWh of energy savings per run. Note that these energy savings are per simulation run, and will compound over the lifetime of the machine, potentially helping to defray the cost of the initial deployment. Although analysis nodes offer increased performance, they are seen to consume more energy at low staging ratios than offline processing, as they spend significant time idle; this idle time (and energy expenditure) is reduced at higher staging ratios.

Inference: *Overall, active flash makes data analysis virtually “free” in most cases when it is piggybacked on the SSDs, because performing computation at SSD controller avoids the infrastructure cost of analysis or offline*

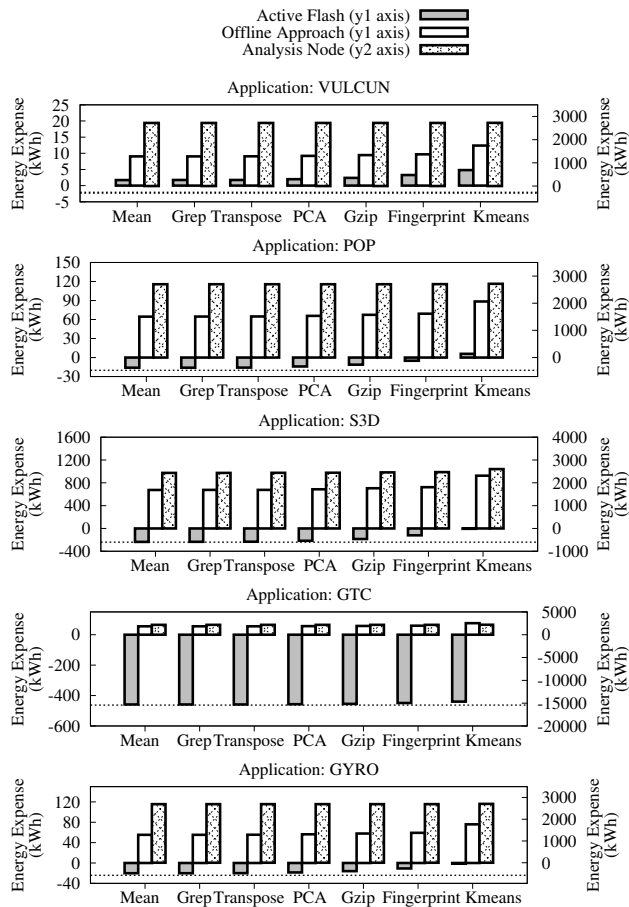


Figure 4: Comparing the energy expenses of all applications for Active Flash, offline, and analysis nodes techniques. Expenses are w.r.t. running only the simulation job using PFS, without SSDs ($baseline_{PFS}$). Dotted line denotes energy savings due to running only simulation using SSDs without active computation ($baseline_{SSD}$). Active flash and offline are plotted on the primary y-axis (y1), and the analysis nodes model is plotted on the secondary y-axis (y2).

nodes, and also results in performance improvement and energy savings.

Overall cost: To better understand the overall costs we examine active flash and analysis nodes (both of which offer better performance than offline) at various staging ratios (Table 2) across our portfolio of HPC applications, comparing the up-front (capital) costs as well as the energy expenditure over time. We study the trade-off between these costs, displaying infrastructure and 2-year energy costs in Table 5 for running our application portfolio continuously at staging ratios of 10, 30, and 300.

At a staging ratio of 10, both active flash, and analysis nodes can support all of the application/kernel combinations. In Table 5 we see that active flash is the most energy-efficient, saving \$19,131 (at \$0.30 per kWh) to support the five applications for a period of two years and

thereby defraying almost 11% of the deployment cost of \$180,000. In contrast, the analysis node approach results in energy costs of \$566,375, or an additional 31% on top of the initial provisioning cost of \$1,818,000.

At staging ratios of 30 and 300 active flash cannot be used with any applications, while analysis nodes are more cost effective, while failing to run *GTC* (at 30 and 300) and *S3D* (at 300). At a ratio of 30 the infrastructure and energy expenses decrease to roughly \$606,000 and \$158,193, respectively; at 300 the infrastructure and energy expenses decrease even further to roughly \$60,600 and \$31,072, respectively.

Inference: Energy costs for analysis nodes decrease at higher staging ratios, but may not support certain applications, and the cost reduction fails to defray any of the initial infrastructure expense, unlike active flash.

Staging Ratio	Infrastructure Cost (\$)	Energy Bill (\$)	Total Cost (\$)	Feasible Applications
Active Flash Model				
10	180,000	-19,131	160,866	all
30 & 300	-	-	-	none
Analysis Node Model				
10	1,818,000	566,375	2,384,375	all
30	606,000	158,193	642,993	all, w/o GTC
300	60,600	31,072	67,432	all, w/o GTC, S3D

Table 5: Capital and energy costs to support a portfolio of five leadership applications for 2 years. Assumptions: continuous usage, equal number (146) of 24-hour simulation runs per application, electricity \$0.30 per kWh.

Summary of results: In summary, for most of the applications, and all of the analysis kernels, active flash is effective at low staging ratios, while being efficient in terms of both deployment cost and energy; however for higher staging ratios it is unable to support certain applications. Active flash is limited by the bandwidth and write endurance constraints. In contrast, analysis node performs well at higher staging ratios, especially for compute-intensive analytics kernels; however it is limited by capacity constraints on DRAM and suffers from higher cost and energy consumption. A hybrid approach, deploying analysis nodes with active flash might be feasible, but is beyond the scope of this paper.

6 Active Flash Prototype

To demonstrated feasibility of the active flash approach, we have implemented a prototype on the Jasmine OpenSSD development platform [26], extending the OpenSSD flash translation layer (FTL) with data analysis functions. This platform uses the Indilinx Barefoot controller, an ARM-based SATA controller with parameters shown in Table 6.

An overview of our implementation is shown in Figure 5. Active flash functionality is requested via out-of-band commands, distinguished by LBA range. An active flash operation comprises: **(a) write:** analysis input

Parameter	Value
Controller	ARM Indilinx Barefoot™ at 87.5 MHz
Host Interface	SATA 2 at 3 Gbps
SDRAM	64 MB
Flash Memory	64 GB

Table 6: SSD parameters on the OpenSSD platform.

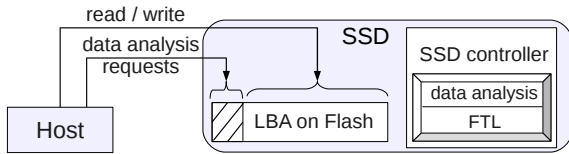


Figure 5: Active Flash prototype.

data is written by the host to the SSD, e.g. as part of a checkpoint operation, **(b) request:** data analysis request sent in the form of write to a reserved LBA, **(c) process:** the analysis kernel running on the SSD controller, reading input data from internal flash (where it was written in step (a)), **(d) result:** output data is written to internal SSD storage, and the host notified via polling or completion of a pending command.

6.1 Data analysis commands

The command format is simple and general, as shown in Figure 6, specifying an operation, a list of LBA extents, and operation-specific options.

Data for analysis is transferred to the controller by (a) writing to a file in the host file system, (b) flushing data from RAM to storage, (c) translating offsets within the file into physical LBAs, and (d) passing the sequence of LBA extents in the analysis command. Analysis results are returned by creating and pre-allocating a file for analysis output, then again translating file offsets to LBAs and passing an LBA extent list to the controller.

Simple analysis requests such as the statistical kernels described below (mean, max, standard deviation, linear regression) are fully specified by the command type; input is retrieved from the locations identified in the extent list. A variable-length options field is available for more sophisticated kernels like K-means clustering, which may require additional parameters.

The analysis input typically represents a multi-dimensional numeric array; in the current implementation this data layout is either known implicitly by the analysis kernel or is specified in the Options field. In practice this information is expected to be conveyed via the use of self-describing data formats such as NetCDF [41] or HDF5 [25]: metadata in these scientific data storage formats include information such as array shape and precision needed to interpret the raw data.

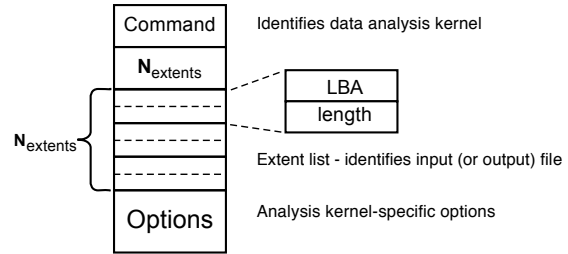


Figure 6: Data analysis command format.

6.2 Scheduling I/O and data analysis tasks

As part of servicing read and write requests, SSD controllers must perform a number of overhead functions, such as garbage collection, wear leveling, bad block management, and error correction-related tasks. Some of these are performed at request time, while others may be deferred to background processing. In either case, such tasks will compete for CPU time with analysis tasks. To minimize impact on SSD performance on our single-core prototype, we implement a preemption-based scheme: data analysis is interrupted when I/O requests arrive, resuming after they finish.

The OpenSSD-based prototype implements a simple event loop, with CPU-bound tasks processed to completion. This preemption is performed by polling for requests at periodic intervals, implemented by processing B bytes at a time between checks. I/O requests may thus have to wait until the current interval is finished, incurring a mean delay of half that interval. Suppose $T_{SSD,k}$ is the throughput of the data analysis kernel k , this delay is:

$$Delay_k = \frac{1}{2} \cdot \frac{B}{T_{SSD,k}}$$

In our prototype B is currently set to 32 KB, the hardware flash controller read size; for the analysis kernels shown in Table 7 below, this results in a mean delay of 3 to 8 ms. When I/O service requests are received in bursts, this delay should only be incurred once, achieving an acceptably low level of interference; on multi-core SSDs it may be avoided entirely.

6.3 Results

The host-controller communication mechanism described above, plus four data analysis kernels, have been implemented in our prototype as part of the SSD firmware. The kernels represent statistical computation common for scientific data processing: max, mean, standard deviation and linear regression. Input for all experiments consisted of 100 MB of 32-bit integers, stored on the SSD in binary. For comparison, each kernel computation was performed on the host CPU, an AMD Phenom 9550 quad-core at 2200 MHz with 2 GB of DRAM.

Throughput: Analysis throughput is shown in Table 7. We see that the statistical data analysis kernels

Data analysis kernel	Throughput (MB/s)		Time (s)				Energy (Joules)	
	Active Flash	Host	Active Flash I/O	Host compute	Active Flash I/O	Host compute	Active Flash	Host
Max	4.5	33.3	2.4	19.8	2.6	0.4	31	288
Mean	4.0	33.1	2.4	22.1	2.6	0.4	34	290
Standard Deviation	3.3	32.0	2.4	27.7	2.6	0.5	42	300
Linear Regression	1.9	26.8	2.4	49.6	2.6	1.1	73	357

Table 7: Performance of data analysis kernels on active flash controller and host: throughput, I/O and computation time, and energy consumption. Input size = 100 MB; host CPU = AMD 2200 MHz, active flash CPU = ARM 87.5 MHz

achieve about 2–4.5 MB/s on the SSD controller (second column), and run about 7–14 times faster on the host CPU (third column). The OpenSSD CPU runs at only 87.5 MHz; active flash performance is expected to scale with faster cores in today’s higher-end SSDs (e.g. the OCZ RevoDrive X2, with four 780 MHz Tensilica cores).

Division of I/O and computation time: Analysis run time consists of I/O and computation:

$$t = t_{io} + t_{comp} \quad (35)$$

For active flash, $t_{io} = t_{fm2c} + t_{c2m}$ represents the time to read the data from flash to the controller’s DRAM. For host-resident data analysis, $t_{io} = t_{fm2host}$ is the time to read the data from flash to the DRAM on host.

In Table 7 I/O and computation time is presented in each case for 100 MB of input data; as expected, with active flash, t_{comp} is dominant, while the host-resident analysis time is dominated by t_{io} . Since the controller is optimized to deliver full internal flash bandwidth to the host, the two cases generated very similar I/O time with 32 KB reads. However, if less well-aligned read sizes are used by the host application, the SSD-to-host I/O time will increase (e.g., to 9 seconds with 4 K reads).

Power and energy consumption: The active flash prototype and host were measured in idle (1.35 W, 79 W), sustained write (1.5 W, 80 W) and data analysis (1.4 W, 96 W) states. Note that the relatively flat power consumption of OpenSSD is typical of low-end CPUs; higher-end embedded cores may incorporate power-saving idle modes similar to those of the host CPU. Energy consumption for processing 100 MB of data is also shown in Table 7; the active flash prototype is seen to use 5 to 9 times less energy than host-resident processing.

7 Related Work

Active Disk [42] and IDISK [27] were early proposals for shifting computation to the disk-resident CPU, with target applications including image processing and data filtering. Active storage concepts have been explored in the context of PFS [39, 43], where the computation is performed on the I/O nodes. Kim et al. [20] studied the feasibility of offloading database scan operations on the SSD controller. Cho et al. [17] have proposed hardware changes (adding reconfigurable stream processors) to the SSD for offloading data-intensive tasks. In

contrast, our approach does not require any hardware changes. Boboila et al. have proposed *Active Flash* [13], which takes advantage of the higher internal bandwidth and lower power; Boboila’s work, however, models a single active flash device rather than a workflow. In contrast, we evaluate the active computation paradigm on SSDs in a supercomputing environment for a class of HPC simulations and data analyses (preliminary results appeared here [44]). Additionally, in comparison to prior work, we are unique in considering a case where data output rates impose real-time constraints on active computation to avoid overall performance degradation.

8 Conclusion

We have proposed active flash, an approach to perform in-situ scientific data analysis on SSDs, in HEC machines. We have presented detailed performance and energy models for active flash, offline, and analysis nodes, and studied their provisioning cost, performance, and energy consumption. Our modeling and simulation results indicate that active flash is better than the other approaches in helping to reduce both data movement, and energy consumption, while also improving the overall application performance. Interestingly, our results suggest that active flash can even help defray part of the capital expenditure through energy savings. Further, we have demonstrated the feasibility of active flash through the construction of a prototype, based on the OpenSSD development platform, extending the OpenSSD FTL with data analysis functions. Finally, our experience suggests that active flash is a viable, cost-effective approach for future in-situ scientific data analysis.

9 Acknowledgments

We thank the reviewers and our shepherd, Erik Riedel, for their constructive comments. This research was supported in part by, and used the resources of, the Oak Ridge Leadership Computing Facility, located in the National Center for Computational Sciences at ORNL, which is managed by UT Battelle, LLC for the U.S. DOE (under the contract No. DE-AC05-00OR22725). It was also supported in part by NSF awards CCF-1116540, CNS-0915861, CCF-0937690 and CNS-1149232, an IBM Faculty Award, and Xiaosong Ma’s joint appointment between NCSU and ORNL.

References

- [1] Computational science requirements for leadership computing, 2007, <http://tinyurl.com/nccs2007>.
- [2] DDR3 Memory price 64GB(8x8). <http://tinyurl.com/dramprice>.
- [3] Intel core i7-2600 processors. <http://ark.intel.com/products/52213>.
- [4] Micron dram datasheet. <http://tinyurl.com/drambw>.
- [5] Processor price (Intel Core i7-2600). <http://ark.intel.com/products/52213>.
- [6] Samsung pm830 datasheet. <http://tinyurl.com/co9zyq7>.
- [7] SSD price (Samsung 830 Series 64GB). <http://tinyurl.com/9cldame>.
- [8] National Center for Computational Sciences. <http://www.nccs.gov/>, 2008.
- [9] Scientific Grand Challenges. Architectures and Technology for Extreme Scale Computing. Technical report, Dec 2009.
- [10] Samer Al-Kiswany, Matei Ripeanu, Sudharshan S. Vazhkudai, and Abdullah Gharaibeh. stdchk: A Checkpoint Storage System for Desktop Grid Computing. In *ICDCS'08*.
- [11] D.G. Andersen, J. Franklin, M. Kaminsky, A. Phanishayee, L. Tan, and V. Vasudevan. Fawn: A fast array of wimpy nodes. In *Proceedings of the ACM SIGOPS 22nd symposium on Operating systems principles*, pages 1–14. ACM, 2009.
- [12] Leonardo Bautista-Gomez, Seiji Tsuboi, Dimitri Komatitsch, Franck Cappello, Naoya Maruyama, and Satoshi Matsuoka. Fti: high performance fault tolerance interface for hybrid systems. In *Proceedings of 2011 International Conference for High Performance Computing, Networking, Storage and Analysis*, SC '11, pages 32:1–32:32, New York, NY, USA, 2011. ACM.
- [13] Simona Boboila, Youngjae Kim, Sudharshan Vazhkudai, Peter Desnoyers, and Galen Shipman. Active flash: Performance-energy tradeoffs for out-of-core processing on non-volatile memory devices. In *Proceedings of the 2012 IEEE 26th Symposium on Mass Storage Systems and Technologies (MSST)*, MSST '12, April 2012.
- [14] Shekhar Borkar. Technology and Design Challenges to Realize Exascale. Intel Corp. <http://www.orau.gov/archI2011/presentations/borkars.pdf>, Aug 2011.
- [15] G. Bronevetsky and A. Moody. Scalable i/o systems via node-local storage: Approaching 1 tb/sec file i/o. LLNL Technical Report LLNL-TR-415791, Lawrence Livermore National Laboratory, 2009.
- [16] P. Carns, K. Harms, W. Allcock, C. Bacon, S. Lang, R. Latham, and R. Ross. Understanding and improving computational science storage access through continuous characterization. *ACM Transactions on Storage (TOS)*, 7(3):8, 2011.
- [17] S. Cho, C. Park, H. Oh, S. Kim, Y. Yi, and G.R. Ganger. Active disk meets flash: A case for intelligent ssds. 2011.
- [18] William James Dally and Brian Towles. Principles and Practices of Interconnection Networks. *Morgan Kaufmann Publishers, Inc. ISBN 978-0-12-200751-4*, 2004.
- [19] David Dillow, Galen M Shipman, Sarp Oral, Zhe Zang, and Youngjae Kim. Enhancing i/o throughput via efficient routing and placement for large-scale parallel file systems. In *Proceedings of the 30th IEEE Int'l Performance Computing and Communications Conference*, IPCCC '11, pages 1–9, 2011.
- [20] Kim et al. Fast, Energy Efficient Scan inside Flash Memory Solid-State Drives. In *the International Workshop on Accelerating Data Management Systems (ADMS) with VLDB*, 2011.
- [21] Ranger et al. Evaluating mapreduce for multi-core and multiprocessor systems. In *HPCA*, 2007.
- [22] Zheng et al. Predata - preparatory data analytics on peta-scale machines. In *IPDPS*, 2010.
- [23] Gnu grep, <http://www.gnu.org/software/grep/>.
- [24] Gnu zip, <http://www.gzip.org/>.
- [25] HDF Group. Hierarchical data format, version 5. <http://hdf.ncsa.uiuc.edu/HDF5>.
- [26] Jasmine OpenSSD Platform. <http://www.openssd-project.org>.
- [27] Kimberly Keeton, David A. Patterson, and Joseph M. Hellerstein. A case for intelligent disks (idisks). *SIGMOD Rec.*, 27(3):42–52, 1998.

- [28] Y. Kim, R. Gunasekaran, G.M. Shipman, D.A. Dillow, Z. Zhang, and B.W. Settlemyer. Workload characterization of a leadership class storage cluster. In *Petascale Data Storage Workshop (PDSW), 2010 5th*, pages 1–5. IEEE, 2010.
- [29] ExaScale Computing Study: Technology Challenges in Achieving Exascale Systems, Peter Kogge, Editor and Study Lead, 2008.
- [30] N. Mi, A. Riska, E. Smirni, and E. Riedel. Enhancing data availability in disk drives through background activities. In *Dependable Systems and Networks With FTCS and DCC, 2008. DSN 2008. IEEE International Conference on*, pages 492–501. IEEE, 2008.
- [31] N. Mi, A. Riska, Q. Zhang, E. Smirni, and E. Riedel. Efficient management of idleness in storage systems. *Trans. Storage*, 5(4):1–4, 2009.
- [32] Michael L. Norman and Allan Snaveley. Accelerating Data-intensive Science with Gordon and Dash. In *TG'10*.
- [33] OCZ RevoDrive PCI-Express SSD Specifications. <http://www.ocztechnology.com/ocz-revodrives-pci-express-ssd.html>.
- [34] U.S. Department of Energy. DOE exascale initiative technical roadmap, December 2009. <http://extremecomputing.labworks.org/hardware/collaboration/EI-RoadMapV21-SanDiego.pdf>.
- [35] Sarp Oral, Feiyi Wang, David Dillow, Galen Shipman, Ross Miller, and Oleg Drokin. Efficient object storage journaling in a distributed parallel file system. In *Proceedings of the 8th USENIX conference on File and storage technologies, FAST'10*, pages 11–11, Berkeley, CA, USA, 2010. USENIX Association.
- [36] Preparing for Exascale: ORNL Leadership Computing Facility Application Requirements and Strategy, 2009, <http://tinyurl.com/nccs2009>.
- [37] X. Ouyang, S. Marcarelli, and D. Panda. Enhancing Checkpoint Writing with Staging IO and SSD. In *In Workshop on Storage Network Architecture and Parallel I/Os (SNAPI'10)*, May 2010.
- [38] The Pandaboard Development System. <http://pandaboard.org/>.
- [39] Juan Piernas, Jarek Nieplocha, and Evan J. Felix. Evaluation of active storage strategies for the lustre parallel file system. In *Proceedings of the 2007 ACM/IEEE conference on Supercomputing, SC '07*, pages 28:1–28:10, 2007.
- [40] Ramya Prabhakar, Sudharshan S. Vazhkudai, Youngjae Kim, Ali R. Butt, Min Li, and Mahmut Kandemir. Provisioning a multi-tiered data staging area for extreme-scale machines. In *Proceedings of the 2011 31st International Conference on Distributed Computing Systems, ICDCS '11*, pages 1–12, 2011.
- [41] R. Rew and G. Davis. NetCDF: an interface for scientific data access. *IEEE Comput. Graph. Appl.*, 10(4):76–82, 1990.
- [42] Erik Riedel, Garth A. Gibson, and Christos Faloutsos. Active storage for large-scale data mining and multimedia. In *Proceedings of the 24rd International Conference on Very Large Data Bases, VLDB '98*, pages 62–73, 1998.
- [43] Seung Woo Son, Samuel Lang, Philip Carns, Robert Ross, Rajeev Thakur, Berkin Ozisikyilmaz, Prabhat Kumar, Wei-Keng Liao, and Alok Choudhary. Enabling active storage on parallel i/o software stacks. In *Proceedings of the 2010 IEEE 26th Symposium on Mass Storage Systems and Technologies (MSST), MSST '10*, pages 1–12, Washington, DC, USA, 2010. IEEE Computer Society.
- [44] D. Tiwari, S.S. Vazhkudai, Y. Kim, X. Ma, S. Boboila, and P.J. Desnoyers. Reducing data movement costs using energy-efficient, active computation on ssd. In *Proceedings of the 2012 USENIX conference on Power-Aware Computing and Systems*. USENIX Association, 2012.
- [45] Top500 supercomputer sites. <http://www.top500.org>.